Journal of Oceanology and Limnology
Vol. 39 No. 6, P. 2209-2219, 2021
https://doi.org/10.1007/s00343-021-0297-5

Adsorption of Th and Pa onto particles and the effect of organic compounds in natural seawater*

Xinxing ZHANG[1, 2], Weifeng YANG[1, 3, **], Yusheng QIU[1], Minfang ZHENG[1]

[1] *College of Ocean and Earth Sciences*, *Xiamen University*, *Xiamen 361102*, *China*

[2] *North China Sea Environmental Monitoring Center*, *State Oceanic Administration*, *Qingdao 266033*, *China*

[3] *State Key Laboratory of Marine Environmental Science*, *Xiamen 361102*, *China*

Received Aug. 1, 2020; accepted in principle Nov. 25, 2020; accepted for publication Dec. 24, 2020

Abstract ^{231}Pa and ^{230}Th are two crucial isotopes in the ongoing GEOTRACES Project. However, the controversy on ^{231}Pa/^{230}Th proxy pertaining to archiving ocean circulation or recording paleoproductivity, is still unresolved, partly owing to the unclear understanding of fractionation between ^{231}Pa and ^{230}Th during adsorption. In this study, controlled experiments were conducted to examine the adsorption of ^{234}Th and ^{233}Pa onto biogenic particles (SiO_2 and $CaCO_3$), authigenic minerals (MnO_2 and Fe_2O_3), and lithogenic minerals (kaolinite, attapulgite, montmorillonite, and aluminum oxyhydroxides), and the role of organic compounds in regulating the adsorption of ^{234}Th and ^{233}Pa in natural seawater was evaluated. The distribution coefficients (K_d, presented as logK_d) varied from 3.56 to 6.05 and from 3.27 to 5.82 for ^{234}Th and ^{233}Pa, respectively. Fe_2O_3 is the strongest sorbent for both ^{234}Th and ^{233}Pa. Most of the particles showed comparable logK_d values for either ^{234}Th (~4.8) or ^{233}Pa (~3.9) in the presence of dextran, indicating that the adsorption of Th and Pa is likely controlled by organic coating on particle surfaces. The fractionation factors ($F_{Th/Pa}$) of SiO_2 (3±1) and $CaCO_3$ (33±1) suggest in situ observed preferential scavenging of ^{230}Th to ^{231}Pa in the surface water of low- to mid-latitude regions and the nearly equal removal in the Antarctic Ocean where biogenic silica dominates the particle regime. The $F_{Th/Pa}$ values of the lithogenic and biogenic particles indicate that ^{230}Th is scavenged prior to ^{231}Pa in the particle-scarce ocean interior. The equal scavenging of ^{230}Th and ^{231}Pa at the ocean margins and the ridge crests is dominated by high particle fluxes instead of particle composition control. These results imply that ^{230}Th/^{231}Pa can be used as different proxies in different oceanic settings.

Keyword: thorium; protactinium; paleoproductivity; circulation; particle dynamics

1 INTRODUCTION

^{230}Th and ^{231}Pa are important radionuclides in the ongoing GEOTRACES Project (Pavia et al., 2018; Lerner et al., 2020). In the ocean, the two radionuclides are produced from uranium isotopes. Owing to the even distribution (Lippold et al., 2011) and stable decay of ^{235}U and ^{234}U, the production ratio of ^{231}Pa and ^{230}Th is 0.093 (Lippold et al., 2012). Both Th and Pa are particle-reactive in seawater (Ma et al., 2008; Gdaniec et al., 2018), with Th exhibiting somewhat stronger particle reactivity than Pa (Deng et al., 2018). The removal rate of ^{231}Pa is usually lower than that of ^{230}Th, leading to a longer residence time of ^{231}Pa in the water column (Anderson et al., 1983a, b; Hayes et al., 2013). Therefore, ^{231}Pa is widely distributed along with ocean circulation (Lippold et al., 2011), whereas ^{230}Th is mostly confined within its production location (Gdaniec et al., 2018; Costa et al., 2020). Based on this fractionation during their scavenging, the ^{231}Pa/^{230}Th signal unsupported by the decay of parent U nuclides in sediments was proposed to constrain the ocean circulation (Yu et al., 1996). This signal was used to evaluate the Atlantic meridional overturning circulation strength between the Last Glacial Maximum and the present (Lippold et al., 2012),

* Supported by the National Natural Science Foundation of China (Nos. 42076030, 41476061) and the National Key Basic Research Special Foundation Program of China (No. 2015CB452902)

** Corresponding author: wyang@xmu.edu.cn

Table 1 List of particle types and basic parameters used in the adsorption experiments

Type of particle	Size/molecular weight	Supplementary information
Amorphous SiO_2	Median size 4 μm	Amorphous Si≥95%, SiO_2≥99%
$CaCO_3$	2.5–4 μm	
MnO_2	<5 μm	
Fe_2O_3	<5 μm	
Kaolinite	Median size 6 μm	$Al_2O_3{\cdot}2SiO_2{\cdot}2H_2O$
Attapulgite	Median size 5 μm	$Mg_5Si_8O_{20}(OH)_2(OH_2)_4{\cdot}4H_2O$
Montmorillonite	1–3 μm	$Si_8Al_4O_{20}(OH)_4$
α-Al_2O_3	Median size 3–5 μm	Low activity comparing with other Al_2O_3
β-Al_2O_3	Median size 3–5 μm	More active than α-Al_2O_3
$Al(OH)_3$	<5 μm	
Chitin	Coarse flakes	$(C_8H_{13}NO_5)_n$, polysaccharide
Carrageenan	200 kDa	$C_{24}H_{36}O_{25}S_2$, acid polysaccharide
Humic acid	1 kDa	Sodium-salt
Dextran	40 kDa	$(C_6H_{10}O_5)_n$, polysaccharide

changes in the deep circulation in the northwest and central South Atlantic (Jonkers et al., 2015; Rempfer et al., 2017), and deep-water masses in the southwest Indian Ocean (Thomas et al., 2006) and the Arctic Ocean (Luo and Lippold, 2015). Some researchers have reported that sedimentary $^{231}Pa/^{230}Th$ signals record the opal-dominant paleoproductivity in the Southern Ocean (Anderson et al., 2009; Bradtmiller et al., 2009; Kretschmer et al., 2011) and the Equatorial Pacific (Bradtmiller et al., 2006; Costa et al., 2017). These studies suggest that sedimentary $^{230}Th/^{231}Pa$ contains mixed signals of multiple oceanic processes (Grenier et al., 2019). A controversy regarding the application of $^{231}Pa/^{230}Th$ has emerged in the last decades (Lippold et al., 2011). Hence, a thorough understanding of the differences in ^{230}Th and ^{231}Pa adsorption onto particulate matter is crucial for determining the use of sedimentary $^{231}Pa/^{230}Th$ as a paleo proxy (Hayes et al., 2015).

Previous in situ studies on the role of different particulate components in scavenging ^{230}Th and ^{231}Pa showed contrasting conclusions (Luo and Ku, 1999; Chase et al., 2002), probably because of the complex of particle composition that hinders our understanding. Controlled laboratory experiments revealed that different particle types have very different affinity to ^{230}Th and ^{231}Pa, resulting in fractionation, to varying degrees during their adsorption on particles (Guo et al., 2002). A similar scenario was observed in natural seawater simulation experiments (Geibert and Usbeck, 2004). Later, some experiments proved that colloidal particles play an important role in the adsorption and fractionation of Th and Pa in seawater (Lin et al., 2014, 2015). Moreover, phytoplankton-associated biopolymers bind both Th and Pa (Chuang et al., 2013, 2015b). These available studies suggest that both microparticles and nanoparticles (i.e., colloids) affect the adsorption of ^{230}Th and ^{231}Pa in natural seawater, thereby leading to complex interactions between particulate matter and Th and Pa than previously expected.

In this study, we have examined the adsorption of ^{234}Th and ^{233}Pa on different types of microparticles in seawater, including biogenic (amorphous SiO_2 and $CaCO_3$), lithogenic (kaolinite, attapulgite, montmorillonite, α-Al_2O_3, β-Al_2O_3, and $Al(OH)_3$), and authigenic (MnO_2 and Fe_2O_3) particles. Furthermore, model macromolecular organic compounds (chitin, carrageenan, humic acid, and dextran) were used to determine the binding of organic compounds with ^{234}Th and ^{233}Pa. Dextran (polysaccharide) was used to examine the influence of organic coating on the adsorption of ^{234}Th and ^{233}Pa onto microparticle surfaces. The findings of these controlled experiments further enhance our understanding of the available in situ sedimentary $^{231}Pa/^{230}Th$ datasets.

2 MATERIAL AND METHOD

2.1 Particle selection and seawater preparation

Ten types of inorganic microparticles and four types of organic compounds were used in the sorption experiments (Table 1). Amorphous SiO_2 and $CaCO_3$ represent biogenic silica ($SiO_2{\cdot}xH_2O$) and carbonate, respectively (Yang et al., 2013, 2015b). MnO_2 and Fe_2O_3 were used because iron and manganese can form authigenic minerals in oxidative seawater. Kaolinite, attapulgite, and montmorillonite represent typical lithogenic clay particles, and α-Al_2O_3, β-Al_2O_3, and $Al(OH)_3$ were used to determine whether particles with nearly identical chemical compositions but different structures have distinct affinities to a specific particle-reactive nuclide. All the inorganic particles used in the experiments had comparable sizes (mainly 2–5 μm) to avoid the size effect and enable easy comparison of the composition effect. Chitin, carrageenan, and dextran represent polysaccharides and have been previously used to study the adsorption of Th in seawater (Guo et al., 2002; Chuang et al., 2014, 2015a; Lin et al., 2015). Humic acid represents humic substances (Guo et al., 2002).

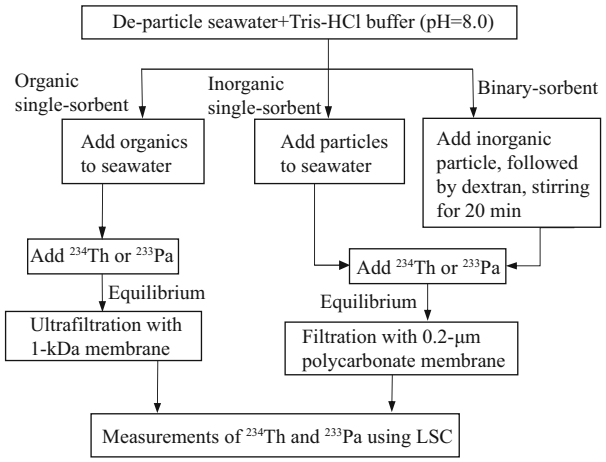

Fig.1 Schematic of the adsorption experiments, including inorganic single-sorbent, organic single-sorbent, and binary-sorbent experiments in natural seawater

LSC denotes liquid scintillation counter.

De-particle and organic seawater was used in the controlled experiments. Natural seawater collected from the South China Sea (salinity 35) was filtered using a precombusted GF/F membrane (Whatman), followed by ultrafiltration using a 1-kDa membrane to remove colloidal particles (Guo et al., 1995). Finally, the seawater was exposed to ultraviolet irradiation for 48 h to decompose residual organic compounds (Lin et al., 2014). Thus, the prepared seawater exhibited characteristics similar to those of natural seawater, except particulate matter was excluded.

2.2 Sorption experiment

The experiments are schematically shown in Fig.1. First, 50 mL of de-particle seawater, including 1 mL of noncomplexing Tris-HCl buffer solution, was added to a stirrer-cell unit to maintain a stable pH and prevent pseudocolloid formation during the addition of spike nuclides (Roberts et al., 2009). For single-sorbent experiments, 2.0 mg of particles were added, resulting in a particle concentration of 40 mg/L, which is comparable to the particle concentrations in some coastal seawater (Chuang et al., 2013; Yang et al., 2013). Then, 400 Bq of ^{234}Th (milked from ^{238}U) or ^{233}Pa (milked from ^{237}Np) were added dropwise while stirring. The pH value was checked before and after spike addition to ensure it remained constant. ^{234}Th or ^{233}Pa were adsorbed on particles for 2 h while stirring to compare our results with previously reported results (Guo et al., 2002; Yang et al., 2013, 2015b; Lin et al., 2014). For inorganic single-sorbent experiments, ^{234}Th or ^{233}Pa in the particulate phase was separated from the dissolved phase via filtration using a 0.2-μm polycarbonate membrane. All the inorganic particles were larger than 1 μm; hence, a 0.2-μm pore size was sufficient for separating the particles from the seawater. Because carrageenan, humic acid, and dextran generally dissolve in seawater, ultrafiltration is often used to separate them from seawater (Chuang et al., 2014, 2015b). In our study, particulate ^{234}Th or ^{233}Pa in the organic single-sorbent experiments was separated via ultrafiltration using a 1-kDa membrane, as performed by Lin et al. (2014, 2015).

For binary-sorbent experiments, after the addition of a type of inorganic particle, 1 mL of dextran solution was added to reach a final concentration of 5 mg/L (Fig.1). The seawater was stirred for 20 min to allow inorganic particles to interact with dextran (Yang et al., 2015b). The procedures were similar to those adopted in inorganic single-sorbent experiments. Since 0.2-μm polycarbonate membrane was used to separate particles from the dissolved phase in binary-sorbent experiments, nuclides left in the dissolved phase included both colloidal and truly soluble species which was similar to natural seawater environment. The obtained partition of nuclides between particles and seawater in the presence of dextran would simulate in situ scenario. In our study, both single- and binary-sorbent experiments were performed in duplicate.

2.3 Measurements of ^{234}Th and ^{233}Pa

The activities of ^{234}Th and ^{233}Pa were counted using a liquid scintillation counter (LSC, Tris-Carb 2900TR, PerkinElmer), as performed by Lin et al. (2014, 2015). All particulate and dissolved samples were dried at 100 °C. Then, 10 mL of the cocktail was added to the samples, and the samples were measured. Within an activity scope of 0–600 Bq, the constant counting efficiency of LSC is 93%. The blank of the scintillation solution was also determined to correct the influence of the background. Samples were counted until a counting error of less than 5% was achieved, depending on their specific activities.

2.4 Distribution coefficient and fractionation factor

The distribution coefficient (K_d) between the particulate and dissolved phases (Honeyman and Santschi, 1989) was used to represent the adsorption of nuclide on various particles. K_d is defined as

$$K_d = \frac{A_P}{A_D \times \mathrm{SPM}}, \quad (1)$$

where A_P and A_D denote the particulate and dissolved

Table 2 LogK_d values (mean±SD) for ^{234}Th and ^{233}Pa of different particles in the absence (single-sorbent experiment) and presence (binary-sorbent experiment) of dextran, and the fractionation factor ($F_{Th/Pa}$) between ^{234}Th and ^{233}Pa during adsorption

Type of particle	^{234}Th		^{233}Pa		$F_{Th/Pa}$	
	Single	Binary	Single	Binary	Single	Binary
Amorphous SiO_2	4.64±0.16	4.60±0.15	5.42±0.57	4.11±0.03	0.2±0.1	3.1±0.1
$CaCO_3$	5.36±0.15	4.91±0.16	4.90±0.01	3.39±0.06	2.9±0.1	33.1±1.3
MnO_2	5.46±0.02	5.06±0.05	4.61±0.01	3.83±0.17	7.1±0.1	16.8±0.8
Fe_2O_3	6.05±0.05	5.30±0.11	5.82±0.01	4.07±0.06	1.7±0.1	17.0±0.4
Kaolinite	4.70±0.72	4.30±0.04	3.74±0.18	4.05±0.25	9.2±1.5	1.8±0.1
Attapulgite	4.97±0.36	5.01±0.62	3.72±0.04	4.17±0.01	17.6±1.3	6.9±0.9
Montmorillonite	4.64±0.32	4.65±0.08	4.06±0.26	4.10±0.14	3.8±0.4	3.5±0.1
α-Al_2O_3	3.56±0.08	4.82±0.15	3.27±0.04	3.68±0.12	1.9±0.1	13.8±0.6
β-Al_2O_3	4.93±0.29	4.90±0.06	3.53±0.48	3.91±0.54	24.8±3.7	9.8±1.4
$Al(OH)_3$	4.66±0.12	4.77±0.33	4.00±0.04	3.84±0.04	4.5±0.1	8.5±0.6
Chitin	5.46±0.13		3.74±0.08		53.1±1.7	
Carrageenan	4.96±0.23		3.46±0.20		31.3±2.3	
Humic acid	5.29±0.11		3.50±0.02		62.4±1.4	
Dextran	5.04±0.52		4.28±0.25		5.8±0.7	

activities of ^{234}Th and ^{233}Pa in Bq/L, respectively. SPM denotes the suspended particulate matter content in kg/L. Thus, K_d is expressed in units of L/kg. To facilitate discussion and comparison with published datasets, logarithmic K_d i.e. logK_d (Table 2) was adopted herein.

Fractionation factor (i.e. $F_{Th/Pa}$) was used to quantify the difference in the affinity of particle types to ^{234}Th and ^{233}Pa, it is defined as

$$F_{Th/Pa} = \frac{K_{d,Th}}{K_{d,Pa}}, \quad (2)$$

where $K_{d,Th}$ and $K_{d,Pa}$ are the distribution coefficients of ^{234}Th and ^{233}Pa, respectively. When $F_{Th/Pa}$ equals 1.0 for a type of particle, this particle has the same affinity to both ^{234}Th and ^{233}Pa; then, no fractionation effect is observed during the adsorption of the two nuclides onto this particle type. Particles with $F_{Th/Pa}$>1 tend to preferentially adsorb ^{234}Th than ^{233}Pa. Particles with $F_{Th/Pa}$<1.0 exhibit greater affinity to ^{233}Pa than to ^{234}Th.

3 RESULT

In the single-sorbent experiments, the log$K_{d,Th}$ values, spanning two to three orders of magnitude, varied from 3.56±0.08 (mean±SD) to 6.05±0.05, on average of 4.98±0.58 (Table 2). The organic matter showed similar log$K_{d,Th}$ values, ranging from 4.96±0.23 to 5.46±0.13 (Fig.2a). Lithogenic particles showed relatively low log$K_{d,Th}$ values of 3.56–4.97

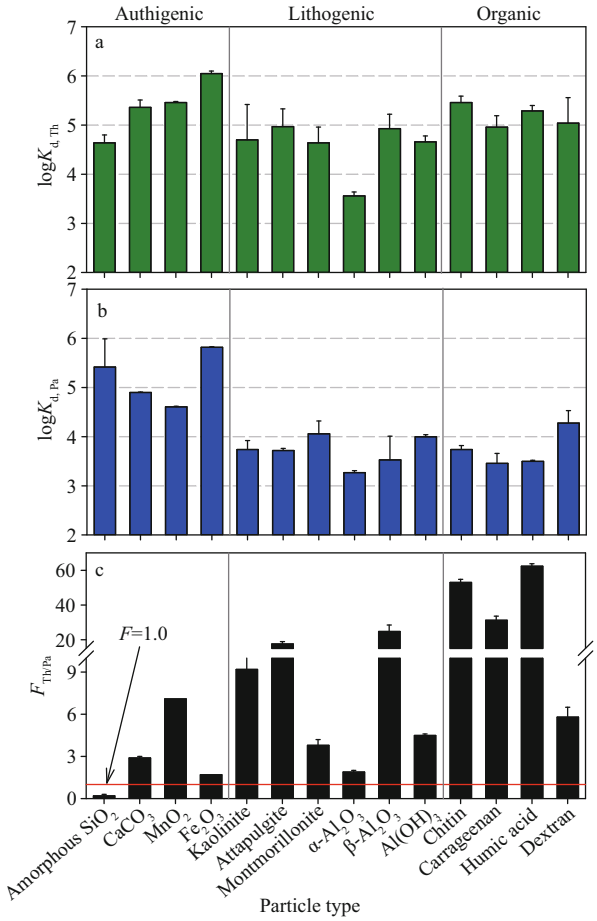

Fig.2 Variations in the logK_d values of ^{234}Th (a) and ^{233}Pa (b) and $F_{Th/Pa}$ (c) values of different particle types in natural seawater

but larger variability of one to two orders of magnitude. The $\log K_{d,\,Th}$ values of biogenic SiO_2, $CaCO_3$, and authigenic MnO_2 and Fe_2O_3 were in the range of 4.64–6.05. In all the experiments, $\log K_{d,\,Pa}$ varied from 3.27 to 5.82 on average of 4.14±0.78 (Fig.2b). Both organic and lithogenic particles exhibited lower variable $\log K_{d,\,Pa}$ values, ranging from 3.27±0.04 to 4.28±0.05. Conversely, biogenic and authigenic particles showed higher $\log K_{d,\,Pa}$ values, varying from 4.61±0.01 to 5.82±0.01. The $F_{Th/Pa}$ values spanned more than two orders of magnitude, varying from 0.2 to 62 on average of 16±20 (Fig.2c). Only for SiO_2, $F_{Th/Pa}$ was less than 1.0. For all other particles, $F_{Th/Pa}$ was greater than 1.0 (Table 2).

In the binary-sorbent experiments, the $\log K_{d,\,Th}$ values varied from 4.30±0.04 to 5.30±0.11, on average of 4.83±0.28 (Table 2), thus showing considerably lesser variability compared with those of pure inorganic particles (i.e., single-sorbent experiments). The $\log K_{d,\,Th}$ values of biogenic and authigenic particles were similar to those of lithogenic particles (4.96±0.29 vs. 4.74±0.25) in the presence of dextran (Fig.3a). For all inorganic particles with dextran, the $\log K_{d,\,Pa}$ values varied from 3.39 to 4.17, on average of 3.91±0.24 (Fig.3b). $CaCO_3$ delivered the lowest $\log K_{d,\,Pa}$ value of 3.39±0.16. The $\log K_{d,\,Pa}$ value of all other particles was approximately 4.0. The $F_{Th/Pa}$ values varied from 2 to 33, on average of 11±9, showing an overall narrow range than that in the single-sorbent experiments (Fig.3c). Notably, $F_{Th/Pa}$>1.0 for all particle types, including SiO_2, in the presence of dextran.

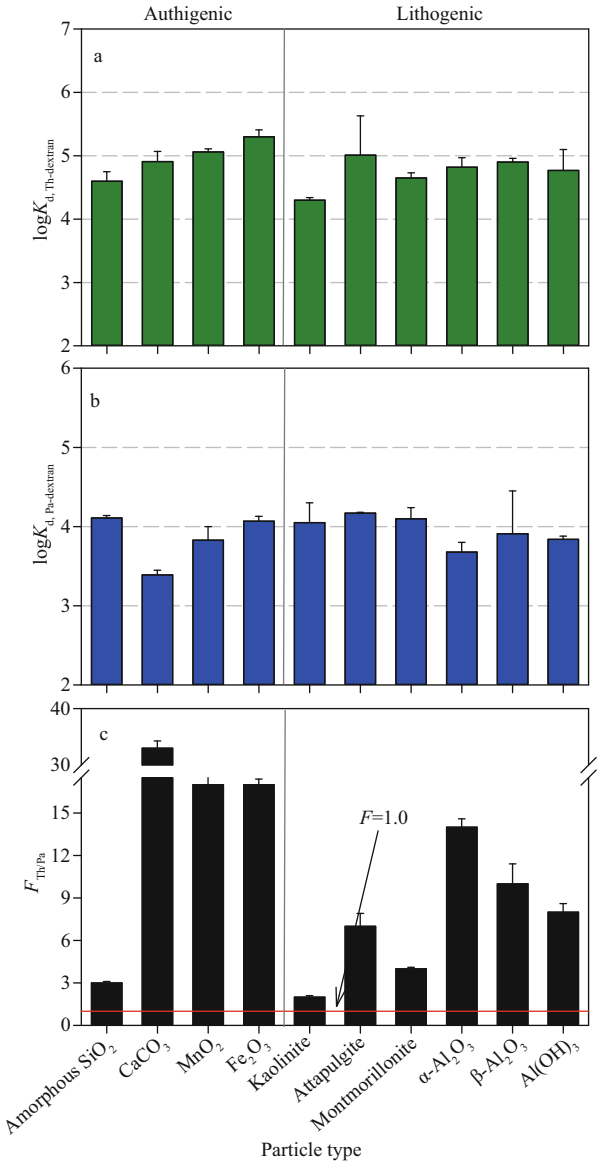

Fig.3 Variations in the $\log K_d$ values of ^{234}Th (a) and ^{233}Pa (b) and $F_{Th/Pa}$ (c) values of different particle types in the presence of dextran

4 DISCUSSION

4.1 Adsorption of organic compounds, SiO_2, and $CaCO_3$

For the four organic compounds considered in this study, the $\log K_{d,\,Th}$ values were nearly consistent, varying from 4.96 to 5.46 (Fig.2a). The main components of chitin, carrageenan, and dextran are polysaccharides (Guo et al., 2002; Yang et al., 2013). Polysaccharides represent the main component of organic matter in seawater (Engel et al., 2004; Chuang et al., 2014, 2015b). Probably, owing to their similar ligands, polysaccharides show comparable affinities to ^{234}Th. The narrow $\log K_{d,\,Pa}$ range (3.46–4.28) also implied the similar affinities of the four organic compounds to ^{233}Pa (Fig.2b). The Martin curve (Martin et al., 1987) indicates that most of the particulate organic matter is confined to the euphotic zone (Yang et al., 2015a, 2016) and the upper mesopelagic water; hence, the microparticulate organic matter absorbing Th and Pa isotopes mainly occurs in the upper oceans. In the deep oceans, organic matter probably affects the adsorption of Th and Pa by means of coating their form on inorganic particles, as observed from the experimental results obtained in the presence of dextran (Fig.3). All types of organic compounds exhibited stronger affinities to Th than to Pa, with $F_{Th/Pa}$>1.0 (Fig.2c).

The $\log K_{d,\,Th}$ value of $CaCO_3$ was higher than that of SiO_2 (Fig.2a); the relation is reversed in the case of ^{233}Pa (Fig.2b). Similar results were reported by Guo et al. (2002). The $F_{Th/Pa}$ values of SiO_2 and $CaCO_3$ were

0.2 and 2.9, respectively. Controlled experiments on nanoparticles also revealed a similar scenario (Lin et al., 2014, 2015). These results indicate that biogenic silica preferentially scavenged Pa over Th, whereas carbonates tended to adsorb Th prior to Pa. Notably, biogenic silica was the only type of particle that preferentially adsorbed Pa in our study (Fig.2c). In the presence of dextran, both SiO_2 and $CaCO_3$ exhibited $\log K_{d,\,Th}$ values comparable to those of the single-sorbent systems (Figs.2 & 3). However, dextran significantly weakened the adsorption of ^{233}Pa on both SiO_2 and $CaCO_3$ particles (Fig.3). The $\log K_{d,\,Pa}$ values decreased from 5.42 to 4.11 and from 4.90 to 3.39 for SiO_2 and $CaCO_3$, respectively (Table 2). Consequently, SiO_2 and $CaCO_3$ showed higher $F_{Th/Pa}$ values than the single-sorbent systems (Fig.3c). Thus, dextran changed the priority of Pa and Th adsorption on SiO_2. Lin et al. (2015) observed similar changes in the case of SiO_2 in the presence of humic acid and acid polysaccharide. Dextran was probably coated on the SiO_2 particle surface, thereby largely changing the surface characteristics of SiO_2 as revealed by the adsorption of ^{210}Po, ^{210}Pb, and ^{7}Be onto SiO_2 particles in the presence of organic compounds (Yang et al., 2013, 2015b). Because of the coating effect, SiO_2 adsorbed Pa in a manner more similar to dextran; this inference was supported by the comparable $\log K_d$ values in the single and binary SiO_2 experiments (Figs.2 & 3). Thus, these results indicate that organic compounds influence the adsorption of Th and Pa onto inorganic particles. Conversely, Chuang et al. (2014) reported that biomolecules from diatoms significantly increase the K_d values by one to two orders of magnitude compared with inorganic particles using biogenic SiO_2. The biomolecules are obtained from cultured diatoms, representing fresh organics with abundant ligands (Chuang et al., 2014). In our study, the organic compounds were commercial products, which generally have less ligands. Abundant binding sites in the fresh organics may enhance the sorption of Th and Pa onto inorganic particles. Thus, the contrasting results support the conclusion that functional groups or ligands essentially determine the radionuclide sorption ability of particles (Chuang et al., 2014).

The particle concentrations used in our experiments were considerably higher than those in the open oceans. Hence, our results can mainly be used to represent the coastal and estuary scenarios. Owing to the linear decrease in K_d with an increase in particle concentration (i.e., particle concentration effect, Honeyman and Santschi, 1989), our $\log K_d$ values cannot be compared with the in situ measured values in the open oceans or directly used to discuss the roles of specific particle types in Th and Pa removal. However, the same particle concentration effects were observed for ^{210}Po and ^{210}Pb with the same particle composition (Yang, 2005), indicating that the particle concentration may have similar influences on the adsorption of nuclides with similar particle reactivity. In this study, the K_d ratio between Th and Pa (i.e., $F_{Th/Pa}$) would be little influenced by the particle concentration. Thus, in our study, $F_{Th/Pa}$ was used to determine the fractionation between ^{230}Th and ^{231}Pa in the upper open oceans where diatoms, dinoflagellates, and coccolithophores dominate the particle regime (Chust et al., 2013). The percentage of coccolithophores in the phytoplankton community usually decreases from tropical and subtropical oceans to high-latitudinal oceans (Chust et al., 2013; Tréguer et al., 2018), as reflected by changes in the biogenic silica content from 40% at the Polar Front to 80% in the southeast Weddell Sea (Walter et al., 2001). According to our results (Fig.3c), $F_{Th/Pa}>30$ for $CaCO_3$, whereas $F_{Th/Pa}=3$ for SiO_2 in the presence of organic compounds. Near the Polar Front, both $CaCO_3$ and SiO_2 dominate the scavenging of ^{230}Th and ^{231}Pa; here, the $F_{Th/Pa}$ value reaches 14 (Walter et al., 1997). To the south, the $F_{Th/Pa}$ values decrease with an increase in the biogenic silica content. In the Weddell Sea, biogenic opal dominates the particulate matter (Walter et al., 2001) and the corresponding $F_{Th/Pa}$ value can be very close to that of SiO_2 endmember (i.e., 3±1, Table 2). In fact, the measured in situ $F_{Th/Pa}$ value from the euphotic zone of the surface of the Weddell Sea is approximately 1.7 (Walter et al., 2001). Moran et al. (2002) also reported a decreasing $F_{Th/Pa}$ trend from ~11 near the equator and South Atlantic gyre to ~2 in the Southern Ocean. Thus, our results, based on the interactions between particles and nuclides, suggest composition dominance over the fractionation of ^{231}Pa and ^{230}Th in the surface water of the open oceans and the Antarctic Ocean.

4.2 Lithogenic particle adsorption

In the single-sorbent experiments, the three clay minerals (i.e., kaolinite, attapulgite, and montmorillonite) exhibited comparable $\log K_{d,\,Th}$ (4.64–4.97) and $\log K_{d,\,Pa}$ (3.72–4.06) values (Table 2), implying that various clay particles show similar affinities for Th and Pa isotopes. Notably, both $\log K_{d,\,Th}$ and $\log K_{d,\,Pa}$ of α-Al_2O_3 were discernibly

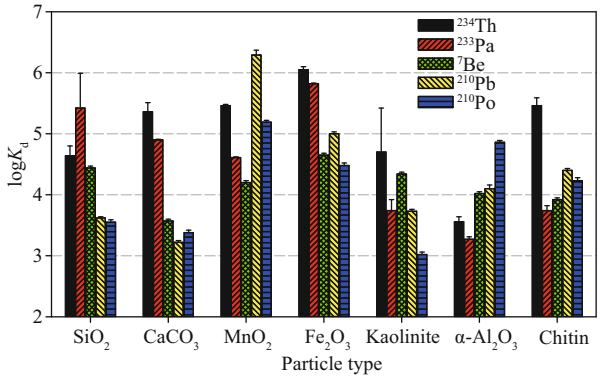

Fig.4 Affinities of various particles to ^{234}Th, ^{233}Pa, ^{7}Be, ^{210}Pb, and ^{210}Po in natural seawater

^{7}Be, ^{210}Po, and ^{210}Pb data are from Yang et al. (2013).

lower, to varying degrees, than those of β-Al_2O_3 and $Al(OH)_3$; this result agrees with the more active nature of β-Al_2O_3 (Table 1). Thus, in addition to the chemical composition, the mineral structure also influences the adsorption characteristics of nuclides on particles. The $F_{Th/Pa}$ values of lithogenic particles varied from 2 to 25 (Fig.2c), indicating their priority for scavenging Th prior to Pa.

In the binary-sorbent experiments, most of the $\log K_{d,\,Th}$ values were approximately 4.8 (Fig.3a), with an exception of kaolinite, which was characterized by a low value of 4.30±0.04. All the $\log K_{d,\,Pa}$ values were comparable and approximately 4. Overall, in the presence of dextran, the $\log K_{d,\,Th}$ values were an order of magnitude higher than the $\log K_{d,\,Pa}$ values (Fig.3a & b), yielding $F_{Th/Pa}$ values of 2–14 (average: 7.4). Overall, $F_{Th/Pa}$ values showed a larger range for the single-sorbent lithogenic particles than for binary-sorbent systems; this large range of values may be ascribed to the differences in either composition or structure (Table 1). In the presence of dextran, the coating effects probably diminished the influence of various lithogenic particles, resulting in synergistic adsorption effects. The $F_{Th/Pa}$ range coincided with the range of the typical fractionation factor of 10 in deep oceans (Anderson et al., 1983a; Walter et al., 1997), implying that the binary-sorbent experiments probably revealed the interaction between the particles and Th and Pa nuclides in the ocean interior. Unlike biogenic silica, lithogenic particles are usually refractory and their percentages in the total particulate matter increase with depth (Brewer et al., 1980). The available report on Th adsorption onto lithogenic particles indicates that these particles have considerably less important roles than particulate organic matter and carbonates in the upper ocean (Yang et al., 2009). Conversely, lithogenic particles can be the crucial components for the adsorption of Th and Pa in the ocean interior (Nozaki and Yamada, 1987). Additionally, most ^{230}Th and ^{231}Pa are produced below the euphotic zone (Bacon et al., 1985; Pavia et al., 2018). Thus, generally, the scavenging and fractionation of ^{230}Th and ^{231}Pa in ocean interior can be closely related to lithogenic particles. Most ^{230}Th produced by ^{234}U decay in the open ocean interior is locally removed by adsorption, whereas less than 50% of ^{231}Pa is locally removed, supporting inference of the preferential scavenging of Th over Pa (Anderson et al., 1983b). Using the limited in situ data from the equatorial Pacific Ocean and Atlantic Ocean (Anderson et al., 1983b), the estimated $F_{Th/Pa}$ varies from 3 to 12, which is close to our results. The $F_{Th/Pa}$ values of approximately 10 in the deep central Pacific Ocean (Anderson et al., 1983a) also support the preferential adsorption of ^{230}Th. In the ordinary deep Pacific Ocean and Atlantic Ocean, the high unsupported ^{230}Th/^{231}Pa ratios in sediments are attributed to the less efficient removal of ^{231}Pa over ^{230}Th (Yang et al., 1986). All these in situ datasets agree with our results. They support the expectation that inorganic particles and organic compounds jointly determine the fractionation between ^{230}Th and ^{231}Pa rather than inorganic components alone (Li, 2005).

4.3 Authigenic Fe and Mn oxyhydroxide adsorption

In the single-sorbent experiments, Fe_2O_3 showed the highest $\log K_{d,\,Th}$ (6.05) and $\log K_{d,\,Pa}$ (5.82) values among all the studied particle types (Fig.2). Further, Fe_2O_3 and MnO_2 exhibited higher $\log K_{d,\,Th}$ and $\log K_{d,\,Pa}$ values than other clay minerals and Al oxyhydroxides. Under similar experimental conditions, both Fe_2O_3 and MnO_2 showed stronger affinities to particle-reactive ^{210}Pb and ^{210}Po than kaolinite and α-Al_2O_3 (Fig.4). A similar scenario was observed in the case of Fe_2O_3 nanoparticles (Lin et al., 2014; Yang et al., 2015b). Thus, Fe and Mn oxyhydroxides seem to be the most effective nonbiogenic sorbents for Th, Pa, Pb, and Po in natural seawater. However, $\log K_{d,\,Pa}$ of SiO_2 and $CaCO_3$ were somewhat higher than that of MnO_2 (Fig.2b), in contrast to that of ^{210}Pb and ^{210}Po (Yang et al., 2013). By considering all the results obtained under similar experimental conditions, it is clear that various particles (i.e., biogenic, lithogenic, and authigenic particles) showed very complex affinities to Th, Pa, Pb, Po, and Be, although these radionuclides were all particle-reactive (Fig.4). The $F_{Th/Pa}$ values of pure Fe_2O_3 and MnO_2 were 2±1 and

7±1, respectively, indicating that Fe_2O_3 adsorbed Th and Pa almost equally and that MnO_2 preferentially scavenged Th prior to Pa. Anderson et al. (1983b) reported that $Fe(OH)_3$ adsorbs ^{234}Th and ^{233}Pa with a Th/Pa ratio of 0.95–1.25 and MnO_2 shows a slight preference for ^{234}Th prior to ^{233}Pa with a Th/Pa ratio of 1.13–1.64; these observations are consistent with our results.

In the presence of dextran, the adsorption ability of both Fe_2O_3 and MnO_2 was reduced (Fig.3). The affinities of MnO_2 to Th and Pa were only slightly lower than that of Fe_2O_3. Consequently, the $F_{Th/Pa}$ values (17±1) for Fe_2O_3 and MnO_2 were comparable (Fig.3c). In the presence of dextran, the fractionation between Th and Pa during their adsorption was enhanced compared with that observed for pure Fe_2O_3 and MnO_2 particles (Fig.2). A similar result was observed for Fe_2O_3 in the presence of acid polysaccharide (Lin et al., 2015). However, a weakened fractionation was observed for Fe_2O_3 in the presence of humic acid and protein (Lin et al., 2015). A study reported that the adsorption of Th onto Fe oxides closely depends on the ratio of humic acid to the combined sites of Fe oxides (Reiller et al., 2002). Thus, the synergistic interactions between Fe_2O_3, MnO_2, and organic compounds regulate the fractionation between Th and Pa. Additionally, different organic compounds have different fractionation effects; however, further investigations are required to understand the detailed mechanism. Together with lithogenic particles, the nonbiogenic particles preferentially scavenged Th prior to Pa, with $F_{Th/Pa}$ in the range of 2–17 (Table 2).

Because they are present in trace amounts, generally, very little Fe and Mn oxyhydroxides are observed in seawater, except in the case of seawater over ridge crests near the hydrothermal emanation, e.g., at the East Pacific Rise at 20°S (Shimmield and Price, 1988) and the Mid-Atlantic Ridge (Hayes et al., 2015). Because $F_{Th/Pa}>1.0$ for Fe_2O_3 and MnO_2 in the presence of organic compounds, and other particles also show priority adsorption for Th (Fig.3c), significant fractionation was observed during ^{230}Th and ^{231}Pa scavenging in the presence of Fe and Mn oxyhydroxides. However, the scavenging of ^{230}Th and ^{231}Pa was equally effective during the precipitation of Fe-Mn oxyhydroxide-rich sediments at 20°S, i.e., the East Pacific Rise; this behavior remains unexplained (Shimmield and Price, 1988). Further, fractionation between ^{230}Th and ^{231}Pa during scavenging has not been observed near continental margins (Anderson et al., 1983a; Shimmield et al., 1986). For example, the unsupported $^{231}Pa/^{230}Th$ ratios of approximately 0.5 in the water column (Nozaki and Yamada, 1987) are similar to the ratios of 0.5 observed in the surface sediment of the Japan Sea (Yang et al., 1986). Interestingly, these regions without the fractionation of ^{230}Th and ^{231}Pa also show high sediment accumulation rates (Boström et al., 1973), thus supporting the inference that in addition to particle composition, particle flux is a principle factor influencing ^{230}Th and ^{231}Pa scavenging from the water column (Lao et al., 1993; Lippold et al., 2011; Pavia et al., 2018). Probably, the adsorption capacity of particles for nuclides depends on both their affinity to nuclides and the abundance. Abundance is a dominant factor for scavenging when particles are sufficiently abundant for scavenging nearly all the nuclides, as observed at the ocean margins and ridge crests (i.e., flux domain) (Gdaniec et al., 2018). Under these circumstances, the scavenging of ^{230}Th and ^{231}Pa is only slightly influenced by the particle composition (Nozaki and Nakanishi, 1985). Conversely, affinity can play a predominant role when particles are too scarce for removing all nuclides, as observed in the open ocean (i.e., the composition domain). Thus, the fractionation induced by the particle composition drivers the preferential scavenging of Th prior to Pa.

5 CONCLUSION

Controlled experiments provide valuable information for understanding the adsorption and fractionation of Th and Pa in natural seawater. The comparability between our results and the available in situ $F_{Th/Pa}$ values indicated that the experiments largely mimic the adsorption of Th and Pa onto particulate matter. With the addition of organic compounds, most of the particle types (i.e., biogenic silica and carbonate, authigenic Fe and Mn oxyhydroxides, and lithogenic minerals) tend to show similar adsorption characteristics for Th or Pa, although these particles have significantly different affinities to Th or Pa in the absence of organic compounds. Thus, the synergistic interactions between inorganic particles and organic compounds jointly determine the adsorption of Th and Pa in natural seawater rather than inorganic particles. Our results support the fractionation between ^{230}Th and ^{231}Pa observed in different oceanic settings. In the surface ocean with abundant biogenic particles, silica and carbonate preferentially or equally scavenge ^{230}Th prior to ^{231}Pa depending on their abundance. Generally, the ocean interior with scarce

particles, lithogenic, probably together with residual biogenic particles, results in preferential scavenging of ^{230}Th prior to ^{231}Pa. At the ocean margins and ridge crests with sufficient particles, the total particle flux dominates the equal scavenging of both ^{230}Th and ^{231}Pa rather than the particle composition. These conclusions imply that ^{230}Th/^{231}Pa can be used to constrain different oceanic processes based on the different fractionation mechanisms.

6 DATA AVAILABILITY STATEMENT

The datasets generated in the current study are presented in Tables 1 & 2.

7 ACKNOWLEDGMENT

The authors thank two anonymous reviewers for their insightful suggestions and Dr. Peng LIN for his help during the de-particle seawater preparation.

References

Anderson R F, Ali S, Bradtmiller L I, Nielsen S H H, Fleisher M Q, Anderson B E, Burckle L H. 2009. Wind-driven upwelling in the Southern Ocean and the deglacial rise in atmospheric CO_2. *Science*, **323**(5920): 1443-1448, https://doi.org/10.1126/science.1167441.

Anderson R F, Bacon M P, Brewer P G. 1983a. Removal of ^{230}Th and ^{231}Pa at ocean margins. *Earth and Planetary Science Letters*, **66**: 73-90, https://doi.org/10.1016/0012-821X(83)90127-9.

Anderson R F, Bacon M P, Brewer P G. 1983b. Removal of ^{230}Th and ^{231}Pa from the open ocean. *Earth and Planetary Science Letters*, **62**(1): 7-23, https://doi.org/10.1016/0012-821X(83)90067-5.

Bacon M P, Huh C A, Fleer A P, Deuser W G. 1985. Seasonality in the flux of natural radionuclides and plutonium in the deep Sargasso Sea. *Deep Sea Research Part A. Oceanographic Research Papers*, **32**(3): 273-286, https://doi.org/10.1016/0198-0149(85)90079-2.

Boström K, Kraemer T, Gartner S. 1973. Provenance and accumulation rates of opaline silica, Al, Ti, Fe, Mn, Cu, Ni and Co in Pacific pelagic sediments. *Chemical Geology*, **11**(2): 123-148, https://doi.org/10.1016/0009-2541(73)90049-1.

Bradtmiller L I, Anderson R F, Fleisher M Q, Burckle L H. 2006. Diatom productivity in the equatorial Pacific Ocean from the last glacial period to the present: a test of the silicic acid leakage hypothesis. *Paleoceanography*, **21**(4): PA4201, https://doi.org/10.1029/2006pa001282.

Bradtmiller L I, Anderson R F, Fleisher M Q, Burckle L H. 2009. Comparing glacial and Holocene opal fluxes in the Pacific sector of the Southern Ocean. *Paleoceanography*, **24**(2): PA2214, https://doi.org/10.1029/2008pa001693.

Brewer P G, Nozaki Y, Spencer D W, Fleer A P. 1980. Sediment trap experiments in the deep North Atlantic: isotopic and elemental fluxes. *Journal of Marine Research*, **38**(4): 703-728.

Chase Z, Anderson R F, Fleisher M Q, Kubik P W. 2002. The influence of particle composition and particle flux on scavenging of Th, Pa and Be in the ocean. *Earth and Planetary Science Letters*, **204**(1-2): 215-229, https://doi.org/10.1016/S0012-821X(02)00984-6.

Chuang C Y, Santschi P H, Ho Y F, Conte M H, Guo L D, Schumann D, Ayranov M, Li Y H. 2013. Role of biopolymers as major carrier phases of Th, Pa, Pb, Po, and Be radionuclides in settling particles from the Atlantic Ocean. *Marine Chemistry*, **157**: 131-143, https://doi.org/10.1016/j.marchem.2013.10.002.

Chuang C Y, Santschi P H, Jiang Y L, Ho Y F, Quigg A, Guo L D, Ayranov M, Schumann D. 2014. Important role of biomolecules from diatoms in the scavenging of particle-reactive radionuclides of thorium, protactinium, lead, polonium, and beryllium in the ocean: a case study with *Phaeodactylum tricornutum*. *Limnology and Oceanography*, **59**(4): 1256-1266, https://doi.org/10.4319/lo.2014.59.4.1256.

Chuang C Y, Santschi P H, Wen L S, Guo L D, Xu C, Zhang S J, Jiang Y L, Ho Y F, Schwehr K A, Quigg A, Hung C C, Ayranov M, Schumann D. 2015a. Binding of Th, Pa, Pb, Po and Be radionuclides to marine colloidal macromolecular organic matter. *Marine Chemistry*, **173**: 320-329, https://doi.org/10.1016/j.marchem.2014.10.014.

Chuang C Y, Santschi P H, Xu C, Jiang Y L, Ho Y F, Quigg A, Guo L D, Hatcher P G, Ayranov M, Schumann D. 2015b. Molecular level characterization of diatom-associated biopolymers that bind ^{234}Th, ^{233}Pa, ^{210}Pb, and ^{7}Be in seawater: a case study with *Phaeodactylum tricornutum*. *Journal of Geophysical Research*: *Biogeoscience*, **120**(9): 1858-1869, https://doi.org/10.1002/2015JG002970.

Chust G, Irigoien X, Chave J, Harris R P. 2013. Latitudinal phytoplankton distribution and the neutral theory of biodiversity. *Global Ecology and Biogeography*, **22**(5): 531-543, https://doi.org/10.1111/geb.12016.

Costa K M, Hayes C T, Anderson R F, Pavia F J, Bausch A, Deng F F, Dutay J C, Geibert W, Heinze C, Henderson G, Hillaire-Marcel C, Hoffmann S, Jaccard S L, Jacobel A W, Kienast S S, Kipp L, Lerner P, Lippold J, Lund D, Marcantonio F, McGee D, McManus J F, Mekik F, Middleton J L, Missiaen L, Not C, Pichat S, Robinson L F, Rowland G H, Roy-Barman M, Tagliabue A, Torfstein A, Winckler G, Zho Y X. 2020. ^{230}Th normalization: new insights on an essential tool for quantifying sedimentary fluxes in the modern and quaternary ocean. *Paleoceanography and Paleoclimatology*, **35**(2): e2019PA003820, https://doi.org/10.1029/2019PA003820.

Costa K M, Jacobel A W, McManus J F, Anderson R F, Winckler G, Thiagarajan N. 2017. Productivity patterns in the equatorial Pacific over the last 30,000 years. *Global Biogeochemical Cycles*, **31**(5): 850-865, https://doi.org/10.1002/2016GB005579.

Deng F F, Henderson G M, Castrillejo M, Perez F F, Steinfeldt

R. 2018. Evolution of ^{231}Pa and ^{230}Th in overflow waters of the North Atlantic. *Biogeoscience*, **15**(23): 7299-7313, https://doi.org/10.5194/bg-15-7299-2018.

Engel A, Thoms S, Riebesell U, Rochelle-Newall E, Zondervan I. 2004. Polysaccharide aggregation as a potential sink of marine dissolved organic carbon. *Nature*, **428**(6986): 929-932, https://doi.org/10.1038/nature02453.

Gdaniec S, Roy-Barman M, Foliot L, Thil F, Dapoigny A, Burckel P, Garcia-Orellana J, Masqué P, Mörth C M, Andersson P S. 2018. Thorium and protactinium isotopes as tracers of marine particle fluxes and deep water circulation in the Mediterranean Sea. *Marine Chemistry*, **199**: 12-23, https://doi.org/10.1016/j.marchem.2017.12.002.

Geibert W, Usbeck R. 2004. Adsorption of thorium and protactinium onto different particle types: experimental findings. *Geochimica et Cosmochimica Acta*, **68**(7): 1489-1501, https://doi.org/10.1016/j.gca.2003.10.011.

Grenier M, Francois R, Soon M, Rutgers van der Loeff M, Yu X X, Valk O, Not C, Moran S B, Edwards R L, Lu Y B, Lepore K, Allen S E. 2019. Changes in circulation and particle scavenging in the Amerasian Basin of the Arctic Ocean over the last three decades inferred from the water column distribution of geochemical tracers. *Journal of Geophysical Research*: *Oceans*, **124**(12): 9338-9363, https://doi.org/10.1029/2019JC015265.

Guo L D, Chen M, Gueguen C. 2002. Control of Pa/Th ratio by particulate chemical composition in the ocean. *Geophysical Research Letters*, **29**(20): 1961, https://doi.org/10.1029/2002GL015666.

Guo L D, Santschi P H, Warnken K W. 1995. Dynamics of dissolved organic carbon (DOC) in oceanic environments. *Limnology and Oceanography*, **40**(8): 1392-1403, https://doi.org/10.4319/lo.1995.40.8.1392.

Hayes C T, Anderson R F, Fleisher M Q, Huang K F, Robinson L F, Lu Y B, Cheng H, Edwards R L, Moran S B. 2015. ^{230}Th and ^{231}Pa on GEOTRACES GA03, the U.S. GEOTRACES North Atlantic transect, and implications for modern and paleoceanographic chemical fluxes. *Deep Sea Research Part II*: *Topical Studies in Oceanography*, **116**: 29-41, https://doi.org/10.1016/j.dsr2.2014.07.007.

Hayes C T, Anderson R F, Jaccard S L, François R, Fleisher M Q, Soon M, Gersonde R. 2013. A new perspective on boundary scavenging in the North Pacific Ocean. *Earth and Planetary Science Letters*, **369-370**: 86-97, https://doi.org/10.1016/j.epsl.2013.03.008.

Honeyman B D, Santschi P H. 1989. A Brownian-pumping model for oceanic trace metal scavenging: evidence from Th isotopes. *Journal of Marine Research*, **47**(4): 951-992.

Jonkers L, Zahn R, Thomas A, Henderson G, Abouchami W, Francois R, Masqué P, Hall I R, Bickert T. 2015. Deep circulation changes in the central South Atlantic during the past 145 kyrs reflected in a combined ^{231}Pa/^{230}Th, Neodymium isotope and benthic δ^{13}C record. *Earth and Planetary Science Letters*, **419**: 14-21, https://doi.org/10.1016/j.epsl.2015.03.004.

Kretschmer S, Geibert W, Rutgers van der Loeff M M, Schnabel C, Xu S, Mollenhauer G. 2011. Fractionation of ^{230}Th, ^{231}Pa, and ^{10}Be induced by particle size and composition within an opal-rich sediment of the Atlantic Southern Ocean. *Geochimica et Cosmochimica Acta*, **75**(22): 6971-6987, https://doi.org/10.1016/j.gca.2011.09.012.

Lao Y, Anderson R F, Broecker W S, Hofmann H J, Wolfli W. 1993. Particulate fluxes of ^{230}Th, ^{231}Pa, and ^{10}Be in the northeastern Pacific Ocean. *Geochimica et Cosmochimica Acta*, **57**(1): 205-217, https://doi.org/10.1016/0016-7037(93)90479-G.

Lerner P, Marchal O, Lam P J, Gardner W, Richardson M J, Mishonov A. 2020. A model study of the relative influences of scavenging and circulation on ^{230}Th and ^{231}Pa in the western North Atlantic. *Deep Sea Research Part I*: *Oceanographic Research Papers*, 2020, **155**: 103159, https://doi.org/10.1016/j.dsr.2019.103159.

Li Y H. 2005. Controversy over the relationship between major components of sediment-trap materials and the bulk distribution coefficients of ^{230}Th, ^{231}Pa, and ^{10}Be. *Earth and Planetary Science Letters*, **233**(1-2): 1-7, https://doi.org/10.1016/j.epsl.2005.02.023.

Lin P, Chen M, Guo L D. 2015. Effect of natural organic matter on the adsorption and fractionation of thorium and protactinium on nanoparticles in seawater. *Marine Chemistry*, **173**: 291-301, https://doi.org/10.1016/j.marchem.2014.08.006.

Lin P, Guo L D, Chen M. 2014. Adsorption and fractionation of thorium and protactinium on nanoparticles in seawater. *Marine Chemistry*, **162**: 50-59, https://doi.org/10.1016/j.marchem.2014.03.004.

Lippold J, Gherardi J M, Luo Y M. 2011. Testing the ^{231}Pa/^{230}Th paleocirculation proxy: a data versus 2D model comparison. *Geophysical Research Letters*, **38**(20): L20603, https://doi.org/10.1029/2011GL049282.

Lippold J, Luo Y M, Francois R, Allen S E, Gherardi J, Pichat S, Hickey B, Schulz H. 2012. Strength and geometry of the glacial Atlantic Meridional Overturning Circulation. *Nature Geoscience*, **5**(11): 813-816, https://doi.org/10.1038/NGEO1608.

Luo S D, Ku T L. 1999. Oceanic ^{231}Pa/^{230}Th ratio influenced by particle composition and remineralization. *Earth and Planetary Science Letters*, **167**(3-4): 183-195, https://doi.org/10.1016/S0012-821X(99)00035-7.

Luo Y M, Lippold J. 2015. Controls on ^{231}Pa and ^{230}Th in the Arctic Ocean. *Geophysical Research Letters*, **42**(14): 5942-5949, https://doi.org/10.1002/2015GL064671.

Ma H, Zeng Z, He J H, Chen L Q, Yin M D, Zeng S, Zeng W Y. 2008. Vertical flux of particulate organic carbon in the central South China Sea estimated from ^{234}Th-^{238}U disequilibria. *Chinese Journal of Oceanology and Limnology*, **26**(4): 480-485, https://doi.org/10.1007/s00343-008-0480-y.

Martin J H, Knauer G A, Karl D M, Broenkow W W. 1987. VERTEX: carbon cycling in the northeast Pacific. *Deep Sea Research Part A. Oceanographic Research Papers*, **34**(2): 267-285, https://doi.org/10.1016/0198-0149(87)90086-0.

Moran S B, Shen C C, Edmonds H N, Weinstein S E, Smith J

N, Edwards R L. 2002. Dissolved and particulate ^{231}Pa and ^{230}Th in the Atlantic Ocean: constraints on intermediate/deep water age, boundary scavenging, and ^{231}Pa/^{230}Th fractionation. *Earth and Planetary Science Letters*, **203**(3-4): 999-1014, https://doi.org/10.1016/S0012-821X(02)00928-7.

Nozaki Y, Nakanishi T. 1985. ^{231}Pa and ^{230}Th profiles in the open ocean water column. *Deep Sea Research Part A. Oceanographic Research Papers*, **32**(10): 1209-1220, https://doi.org/10.1016/0198-0149(85)90004-4.

Nozaki Y, Yamada M. 1987. Thorium and protactinum isotope distribution in waters of the Japan Sea. *Deep Sea Research Part A. Oceanographic Research Papers*, **34**(8): 1417-1430, https://doi.org/10.1016/0198-0149(87)90135-X.

Pavia F, Anderson R, Vivancos S, Fleisher M, Lam P, Lu Y B, Cheng H, Zhang P, Edwards R L. 2018. Intense hydrothermal scavenging of ^{230}Th and ^{231}Pa in the deep Southeast Pacific. *Marine Chemistry*, **201**: 212-228, https://doi.org/10.1016/j.marchem.2017.08.003.

Reiller P, Moulin V, Casanova F, Dautel C. 2002. Retention behaviour of humic substances onto mineral surfaces and consequences upon thorium (IV) mobility: case of iron oxides. *Applied Geochemistry*, **17**(12): 1551-1562, https://doi.org/10.1016/S0883-2927(02)00045-8.

Rempfer J, Stocker T F, Joos F, Lippold J, Jaccard S L. 2017. New insights into cycling of ^{231}Pa and ^{230}Th in the Atlantic Ocean. *Earth and Planetary Science Letters*, **468**: 27-37, https://doi.org/10.1016/j.epsl.2017.03.027.

Roberts K A, Xu C, Hung C C, Conte M H, Santschi P H. 2009. Scavenging and fractionation of thorium vs. protactinium in the ocean, as determined from particle-water partitioning experiments with sediment trap material from the Gulf of Mexico and Sargasso Sea. *Earth and Planetary Science Letters*, **286**(1-2): 131-138, https://doi.org/10.1016/j.epsl.2009.06.029.

Shimmield G B, Murray J W, Thomson J, Bacon M P, Anderson R F, Price N B. 1986. The distribution and behaviour of ^{230}Th and ^{231}Pa at an ocean margin, Baja California, Mexico. *Geochimica et Cosmochimica Acta*, **50**(11): 2499-2507, https://doi.org/10.1016/0016-7037(86)90032-3.

Shimmield G B, Price N B. 1988. The scavenging of U, ^{230}Th and ^{231}Pa during pulsed hydrothermal activity at 20°S, East Pacific Rise. *Geochimica et Cosmochimica Acta*, **52**(3): 669-677, https://doi.org/10.1016/0016-7037(88)90329-8.

Thomas A L, Henderson G M, Robinson L F. 2006. Interpretation of the ^{231}Pa/^{230}Th paleocirculation proxy: new water-column measurements from the southwest Indian Ocean. *Earth and Planetary Science Letters*, **241**(3-4): 493-504, https://doi.org/10.1016/j.epsl.2005.11.031.

Tréguer P, Bowler C, Moriceau B, Dutkiewicz S, Gehlen M, Aumont O, Bittner L, Dugdale R, Finkel Z, Iudicone D, Jahn O, Guidi L, Lasbleiz M, Leblanc K, Levy M, Pondaven P. 2018. Influence of diatom diversity on the ocean biological carbon pump. *Nature Geoscience*, **11**: 27-37, https://doi.org/10.1038/s41561-017-0028-x.

Walter H J, Geibert W, Rutgers van der Loeff M M, Fischer G, Bathmann U. 2001. Shallow vs. deep-water scavenging of ^{231}Pa and ^{230}Th in radionuclide enriched waters of the Atlantic sector of the Southern Ocean. *Deep Sea Research Part I*: *Oceanographic Research Papers*, **48**(2): 471-493, https://doi.org/10.1016/S0967-0637(00)00046-7.

Walter H J, Rutgers van der Loeff M M, Hoeltzen H. 1997. Enhanced scavenging of ^{231}Pa relative to ^{230}Th in the South Atlantic south of the Polar Front: implications for the use of the ^{231}Pa/^{230}Th ratio as a paleoproductivity proxy. *Earth and Planetary Science Letters*, **149**(1-4): 85-100, https://doi.org/10.1016/S0012-821X(97)00068-X.

Yang H S, Nozaki Y, Sakai H, Masuda A. 1986. The distribution of ^{230}Th and ^{231}Pa in the deep-sea surface sediments of the Pacific Ocean. *Geochimica et Cosmochimica Acta*, **50**(1): 81-89, https://doi.org/10.1016/0016-7037(86)90050-5.

Yang W F. 2005. Marine Biogeochemistry of ^{210}Po and ^{210}Pb and Their Implications Regarding the Cycling and Export of Particles. Xiamen University, Xiamen, China. p.295-312. (in Chinese with English abstract)

Yang W F, Chen M, Cao J P, Qiu Y S, Zhang R, Ma Q, Tong J L, Yang J H, Yang Z, Lü E. 2009. Influence of particle composition on thorium scavenging in the marginal China Seas. *Acta Oceanologica Sinica*, **28**(2): 45-53, https://doi.org/10.3969/j.issn.0253-505X.2009.02.005.

Yang W F, Chen M, Zheng M F, He Z G, Zhang X X, Qiu Y S, Xu W B, Ma L L, Lin Z Y, Hu W J, Zeng J. 2015a. Influence of a decaying cyclonic eddy on biogenic silica and particulate organic carbon in the Tropical South China Sea based on ^{234}Th-^{238}U disequilibrium. *PLoS One*, **10**(8): e0136948, https://doi.org/10.1371/journal.pone.0136948.

Yang W F, Guo L D, Chuang C Y, Santschi P H, Schumann D, Ayranov M. 2015b. Influence of organic matter on the adsorption of ^{210}Pb, ^{210}Po and ^{7}Be and their fractionation on nanoparticles in seawater. *Earth and Planetary Science Letters*, **423**: 193-201, https://doi.org/10.1016/j.epsl.2015.05.007.

Yang W F, Guo L D, Chuang C Y, Schumann D, Ayranov M, Santschi P H. 2013. Adsorption characteristics of ^{210}Pb, ^{210}Po and ^{7}Be onto micro-particle surfaces and the effects of macromolecular organic compounds. *Geochimica et Cosmochimica Acta*, **107**: 47-64, https://doi.org/10.1016/j.gca.2012.12.039.

Yang W F, Zhang X X, Chen M, Qiu Y S. 2016. Unusually low ^{234}Th in a hydrothermal effluent plume over the Southwest Indian Ridge. *Geochemistry*, *Geophysics*, *Geosystems*, **17**(9): 3815-3824, https://doi.org/10.1002/2016GC006580.

Yu E F, Francois R, Bacon M P. 1996. Similar rates of modern and last-glacial ocean thermohaline circulation inferred from radiochemical data. *Nature*, **379**(6567): 689-694, https://doi.org/10.1038/379689a0.